



IDO Inhibition Facilitates Antitumor Immunity of V γ 9V δ 2 T Cells in Triple-Negative Breast Cancer

Peng Li^{1,2†}, Ruan Wu^{1,2†}, Ke Li^{3†}, Wenhui Yuan^{1,2}, Chuqian Zeng⁴, Yuting Zhang⁴, Xiao Wang^{1,2}, Xinhai Zhu⁵, Jianjun Zhou⁶, Ping Li^{7*} and Yunfei Gao^{1,2*}

¹ Zhuhai Precision Medical Center, Zhuhai People's Hospital (Zhuhai Hospital Affiliated with Jinan University), Jinan University, Zhuhai, China, ² The Biomedical Translational Research Institute, Faculty of Medical Science, Jinan University, Guangzhou, China, ³ Department of Infectious Disease, Guangdong Second Provincial General Hospital, Guangzhou, China, ⁴ The First Affiliated Hospital, Jinan University, Guangzhou, China, ⁵ Department of Oncology, First Affiliated Hospital, Jinan University, Guangzhou, China, ⁶ Research Center for Translational Medicine, Cancer Stem Cell Institute, East Hospital, Tongji University School of Medicine, Shanghai, China, ⁷ Department of Endocrinology, Guangdong Second Provincial General Hospital, Guangzhou, China

OPEN ACCESS

Edited by:

Morten Hansen,
Herlev Hospital, Denmark

Reviewed by:

Zsolt Sebestyén,
University Medical Center Utrecht,
Netherlands
Zoltan Janos Vereb,
University of Szeged, Hungary

*Correspondence:

Yunfei Gao
tyunfeigao@jnu.edu.cn
Ping Li
15665331995@163.com

[†]These authors have contributed
equally to this work

Specialty section:

This article was submitted to
Cancer Immunity
and Immunotherapy,
a section of the journal
Frontiers in Oncology

Received: 11 March 2021

Accepted: 16 June 2021

Published: 22 July 2021

Citation:

Li P, Wu R, Li K, Yuan W,
Zeng C, Zhang Y, Wang X, Zhu X,
Zhou J, Li P and Gao Y (2021) IDO
Inhibition Facilitates Antitumor
Immunity of V γ 9V δ 2 T Cells in
Triple-Negative Breast Cancer.
Front. Oncol. 11:679517.
doi: 10.3389/fonc.2021.679517

Triple-negative breast cancer (TNBC) escape from immune-mediated destruction was associated with immunosuppressive responses that dampened the activation of tumor-infiltrating CD8 and $\gamma\delta$ T cells. TNBC had a higher level of programmed cell death 1-ligand 1 (PD-L1) and indoleamine 2,3-dioxygenase (IDO), compared with other breast cancer subtypes. But, clinical studies have revealed that the response rate of PD-1/PD-L1 antibody for TNBC treatment was relatively low. However, the antitumor responses of human V γ 9V δ 2 T cells or IDO inhibitor in TNBC treatment are unknown. In this study, we found that IDO1 and PD-L1 were highly expressed in TNBC patients. Analysis of the clinical samples demonstrated that V γ 9V δ 2 T cells became exhausted in triple-negative breast cancer patients. And V γ 9V δ 2 T cells combined with α PD-L1 could not further enhance their antitumor responses *in vitro* and *in vivo*. However, V γ 9V δ 2 T cells combined with IDO1 inhibitor 1-Methyl-L-tryptophan (1-MT) or Lindrostat showed substantial inhibitory effects on MDA-MB-231 tumor cells. Finally, we found that IDO1 inhibitor promoted T cell's cytotoxicity by enhancing perforin production. These results converged to suggest the potential application of V γ 9V δ 2 T cells treated with IDO1 inhibitor for TNBC therapy.

Keywords: IDO, $\gamma\delta$ T cell, 1-Methyl-L-tryptophan, perforin, anti-tumor immunity

INTRODUCTION

Triple-negative breast cancer (TNBC; estrogen receptor α , progesterone receptor and HER2 (ERBB2)-negative) is the subtype of breast cancers with poorest prognosis due to lack of targeted therapies (1, 2). Immune checkpoint inhibitors (ICIs), such as programmed cell death-1 (PD-1), programmed cell death 1-ligand 1 (PD-L1), and cytotoxic T lymphocyte-associated antigen-4 (CTLA-4), are considered as promising immunotherapeutic strategies for TNBC patients (3); however, the first-in-human treatment of targeting the PD-1/PD-L1 axis for TNBC in clinical trials showed benefits for only a minority of patients (4). Previous findings showed that breast cancer

patients with higher levels of infiltrating immune cells had more favorable prognoses, specifically with a higher ratio of tumor-infiltrating cytotoxic CD8 T cells (TILs) to immunosuppressive FoxP3⁺ T regulatory cells (T reg) (5). However, a study on breast cancer demonstrated that tumor-infiltrating $\gamma\delta$ T lymphocytes are correlated with a poor prognosis in human breast cancer patients (ER⁺, Her2⁺ positive) (6). Another study showed that $\gamma\delta$ T cells infiltrated into various tumors, including TNBCs (7–9), and they appeared to be prognostically beneficial (10). A possible explanation for this contradictory phenomenon was that accumulation of $\gamma\delta$ TILs in different breast cancer subtypes might be differently involved in microenvironment and resulted in different outcomes, which were mediated by unknown mechanisms.

The cytosolic enzyme indoleamine 2, 3-dioxygenase (IDO) has been regarded as a potential contributor in breast cancer progression (11). Indoleamine 2, 3-dioxygenase is encoded by the *IDO1* gene and is an intracellular enzyme that participates in the rate-limiting step of the catabolism of L-tryptophan (Trp), an important regulator of amino acid metabolism (12). These enzymes catalyze the oxidation of Trp to N-formyl l-kynurenine (Kyn), which is rapidly converted by formamidases to Kyn (13); however, elevated concentrations of Kyn and high plasma Kyn/Trp ratios frequently occur in patients with advanced-stage cancers and are correlated with poor prognoses (14, 15). IDO expression in the tumor environment (TME) has been linked to the induction of multiple tolerogenic immune phenotypes, including the inhibition of effector T cell activation, enhanced infiltration of myeloid-derived suppressor cells (MDSCs), B cell dysfunction and promotion of tumor angiogenesis (16, 17). Triple-negative breast cancer cells also express IDO in the presence of inflammation and T-cell infiltration (18). Inhibiting of IDO activity could be used to restore tumor immunity in humans, by relieving IDO-mediated immune suppression of MSCs in the TME as well as in tumor cells themselves (19). These inhibitory effects might converge to induce cytotoxic T cell's exhaustion and dampen antitumor immunity. Tumor cells adopted many approaches to suppress the antitumor immunity mediated by cytotoxic T cells; these approaches included inducing the expression of T-cell immunoglobulin and mucin-domain containing-3 (Tim-3), T cell immunoreceptor with Ig and ITIM domains (TIGIT), CTLA-4 and reducing CD28 expression on T cells in TME (20–22).

1-Methyl-L-tryptophan (1-MT) is an investigational small molecule inhibitor of the IDO enzyme (23). In preclinical report, the combination treatment of 1-MT and anti-PD-L1 could more effectively activate CD8⁺ T cells and inhibit tumor growth than any single one of them (24). One study demonstrated that the combination of navoximod (IDO inhibitor) and atezolizumab (anti-PD-L1) displayed acceptable safety, and tolerability for patients with advanced cancer (25). However, this work showed that there was no clear evidence for benefit of adding navoximod to atezolizumab. Tumor infiltrating CD8⁺ T lymphocytes are considered as an independent prognostic factor associated with improved patient survival in basal-like

breast cancers, but not in non-basal triple-negative breast cancers, nor in other intrinsic molecular subtypes (26). Recent study suggested that $\gamma\delta$ TILs could be active against breast cancer and other types of tumors (27). Due to their HLA-independent mode of target cell recognition, $\gamma\delta$ T cells have recently attracted substantial interest as potential effector cells in cell-based cancer immunotherapy (28, 29). Therefore, an adoptive $\gamma\delta$ T cell transfer therapy may be one of the most powerful treatments for patients with malignant tumors.

$\gamma\delta$ T cells provide the early source of interferon- γ (IFN- γ) in tumor immunity and have potent cytotoxic property (30). Among the immune cells, $\gamma\delta$ T cells (V γ 9V δ 2) have emerged as a newly discovered prospective candidate for solid tumor therapy in clinical trials (31–33). These cells recognize antigens in an MHC-independent manner (non-MHC restriction) *via* surface receptor NKG2D; clinical studies used allogeneic $\gamma\delta$ T cells from healthy donors, since $\gamma\delta$ T cells from the blood of tumor patients are sometimes difficult to expand *in vitro*. Clinical trial indicated that $\gamma\delta$ T-cell transfer was safe and well tolerated (32). Currently, most tumor immune therapy strategies, such as chimeric antigen receptor T cell therapy (CAR-T), were mainly based on $\alpha\beta$ T cells (CD4, CD8 T) and had been applied in treating refractory pre-B cell acute lymphoblastic leukemia and diffuse large B cell lymphoma (34, 35). CAR-T cell therapy could induce rapid and durable clinical responses, and sometimes was associated with unique acute toxicities, which could be severe or even fatal to patients (36). ICIs blockade improve the efficacy of current immunotherapies, particularly CAR-T cells, which had shown limited success in treating solid tumors (37, 38). Mouse model data also suggested that fludarabine and cyclophosphamide, frequently administered before CD19-CART infusion to improve their antitumor activity, down-regulated IDO expression in B-cell malignancies (39). However, if combination of human cytotoxic $\gamma\delta$ T cells and IDO inhibitor could mediate strong antitumor immunity in TNBC is barely known.

Here, we showed that *IDO1* and *PD-L1* were expressed in TNBC patients, and V γ 9V δ 2 T cells became exhausted. The IDO enzyme inhibitor 1-MT or Lindrostat enhanced the antitumor efficacy of V γ 9V δ 2 T cells for the treatment in MDA-MB-231 tumor model. However, the anti-PD-L1 antibody combined with V γ 9V δ 2 T cells showed no such kind of effects. 1-MT promoted T cell's cytotoxicity by enhancing perforin production. These results converged to suggest a promotive effect of 1-MT in facilitating the cytotoxic activity of V γ 9V δ 2 T cells in TNBC treatment.

MATERIALS AND METHODS

Ethics Statement

All experiment protocols, including breast tissues or isolation of PBMC from peripheral blood samples of triple negative breast cancer and healthy volunteers, were approved by the Institutional Review Board of Jinan University, Guangzhou, P. R. China (approval number, KY-2020-011).

Cell Culture and Reagents

Human breast cancer cells (MCF-7 and MDA-MB-231) were obtained from American Type Culture Collection (ATCC; Manassas, VA, USA). The cells were cultured in RPMI 1640 (Thermo Fisher) or DMEM (Thermo Fisher) medium supplemented with 10% fetal bovine serum (FBS, Thermo Fisher) and 100 U ml⁻¹ penicillin/streptomycin (Thermo Fisher) at 37°C and 5% CO₂.

PBMC Isolation and Vγ9Vδ2 T Cell Culture *In Vitro*

PBMCs were isolated from the healthy volunteers' whole blood (The First Affiliated Hospital of Jinan University), following standard Ficoll–Paque-based (GE Healthcare) density gradient centrifugation protocol. Vγ9Vδ2 T cells were generated with Zoledronate (Sigma-Aldrich) as described (40). Briefly, isolated PBMCs were suspended in RPMI 1640 medium supplemented with 10% FBS, 100 U ml⁻¹ recombinant human interleukin-2 (Peprotech), and zoledronate (50 μM). The PBMCs were seeded into 24 well plates, followed by routine culture procedures for 10 days before further tests. Vγ9Vδ2 T cells were maintained at a cell density of 1×10⁶ ml⁻¹. When ratio of Vγ9Vδ2 T cells out of total CD3⁺ cells reached 90%, they could be used in experiments. Vγ9Vδ2 T cells were characterized with PerCP-conjugated antihuman TCR Vδ2 (BioLegend) and V500-conjugated antihuman CD3 (BD Biosciences) *via* flow cytometry. In some experiments, the Vγ9Vδ2 T cells were further purified by negative selection with EasySep™ Human Gamma/Delta T Cell Isolation Kit (STEM CELL), and the purity of enriched Vγ9Vδ2 T cells was validated by flow cytometry and was generally higher than 98%.

Cytotoxic Assay

Breast cancer cells were first labeled with 0.5 μM green fluorescence dye CFSE (Thermo Fisher), followed by incubation with Vγ9Vδ2 T cells according to the designated E (effector, Vγ9Vδ2 T): T (target, cancer cell) ratios (0:1, 5:1, and 15:1) at 37°C in a humidified atmosphere with 5% CO₂. After 6 hours, cells were harvested and stained with PI (SUNGENE BIOTECH) for 10 minutes at room temperature. The percentage of dead target cells (CFSE⁺ PI⁺) out of the total target cells was identified *via* flow cytometry. In some experiments, breast cancer cells (MCF-7 and MDA-MB-231) and Vγ9Vδ2 T cells were treated with 0.5 mM 1-Methyl-DL-tryptophan (Sigma-Aldrich), 100 nM Linrodostat (Selleck) or with 10 μg ml⁻¹ PD-L1 (CD274) antibody (Selleck) for 6 or 12 hours. Co-incubation meant that residual 1-MT or anti-PD-L1 in the medium was not washed out and remained in the subsequent tumor killing assays.

In Vitro Assays

For apoptosis detection, tumor cell lines (MDA-MB-231, MCF-7) were treated with vehicle, 0.5 mM 1-MT in the presence of RPMI 1640 medium supplemented with 10% fetal bovine serum for 6, or 12 hours. Cells were then harvested and stained with PI

for 15 minutes at room temperature. The percentage of dead target cells (PI⁺) out of the total number of target cells was determined with flow cytometry.

Human Patient Samples

Thirty patients who were diagnosed with breast cancer (TNBC) by pathological examination were recruited from outpatient clinics in the First Affiliated Hospital of Jinan University. The patients' information was shown in **Supplementary Table 1**. Thirty sex- and age-matched healthy volunteers were recruited from the medical staff at the First Affiliated Hospital of Jinan University. PBMCs were isolated from their whole blood, following the standard Ficoll–Paque-based density gradient centrifugation protocol.

Flow Cytometry

Approximately 10⁵ to 10⁶ human Vγ9Vδ2 T cells were incubated with specific antibodies for 20 minutes at 4°C in the dark for cell surface staining. In some experiments, fresh PBMCs from patients and healthy donors were stimulated with 50 ng/mL phorbol 12-myristate 13-acetate (Sigma-Aldrich) and 1 μg/mL ionomycin (Sigma-Aldrich) in the presence of Golgi Stop (BD Biosciences) for 4 hours, then fixed and permeabilized (BD Biosciences) with antibodies for another 40 minutes at 4°C in the dark, all procedures followed the manufacturer's recommendations (BD Biosciences). The following antibodies were used: PerCP-conjugated anti-human TCR Vδ2 (BioLegend), V500-conjugated anti-human CD3 (BD Biosciences), PE-conjugated anti-human CD28 (BioLegend), PE/Cy7-conjugated anti-human CD45RA (BioLegend), APC-conjugated anti-human CD27 (eBioscience), Pacific Blue™-conjugated anti-human CD279 (BioLegend), APC-conjugated anti-human Tim-3 (BioLegend), APC-conjugated anti-human TIGIT (BioLegend), FITC-conjugated anti-human IFN-γ (BioLegend), APC-conjugated anti-human TNF-α (BioLegend), Pacific Blue™-conjugated anti-human granzyme B (BioLegend), PE/Cy7-conjugated anti-human perforin (BioLegend), and PE/Cy7-conjugated anti-human CD314 (BioLegend). PerCP-conjugated anti-human CD8a (BioLegend), FITC-conjugated anti-human Vδ1 (Miltenyi Biotec), Brilliant Violet 421™-conjugated anti-human CD274 (BioLegend), APC-conjugated anti-human MICA/MICB (BioLegend), and PerCP-conjugated anti-human CD4 (BioLegend). All flow cytometry data analysis was conducted with FlowJo (FLOWJO, LLC) software.

Cytokine Secretion Assay

The effector cells (E, Vγ9Vδ2 T cells) were co-cultured with target cells (T, MCF-7, MDA-MB-231) for 6 or 12 hours at an E:T ratio of 1:0, 5:1, 15:1 and the medium supernatant was detected for the levels of cytokine secretion. In some experiments, breast cancer and Vγ9Vδ2 T cells were treated with 0.5 mM 1-Methyl-DL-tryptophan (1-MT) for 6 or 12 hours. The concentration of TNF-α (TB care health), IFN-γ (TB care health), Perforin (Dakewe), and Granzyme B (Dakewe) were detected using enzyme-linked immunosorbent assay.

NOD/Scid Mice Tumor Models and *In Vivo* Assessment

Non/obese diabetic severe combined immunodeficient (NOD-scid) mice were purchased from Beijing Vital River Laboratory Animal Technology Co., Ltd. All mice were fed with autoclaved food and water. All animal protocols were approved by the Jinan University Institutional Laboratory Animal Care and Use Committee (approval number, IACUC-20190115-04). Mice were used between 5 weeks to 8 weeks of age. 5×10^6 MCF-7 or 1×10^6 MDA-MB-231 tumor cells in 200 μ L of phosphate buffer solution (PBS) were subcutaneously injected. Engrafted mice were randomized into four groups (n=5 per group): PBS, V γ 9V δ 2 T cell (V δ 2), α PD-L1 (Selleck), and combination of V γ 9V δ 2 T cells and α PD-L1. At the indicated time for each experiment, 10^7 V γ 9V δ 2 T cells or α PD-L1 antibodies (250 μ g per mice) in 200 μ L of PBS were adoptively systemically transferred into tumor-bearing (50 mm³) mice by tail vein injection. In order to analyze the efficiency of antitumor immunity of V γ 9V δ 2 T cells and α PD-L1, tumor size was recorded until day 39. In the administration of 1-MT in drinking water, 1-MT (Sigma-Aldrich) was prepared at 5 mg ml⁻¹ (pH 9–10) in water as previously described (48). Engrafted mice were randomized into four groups: PBS, V γ 9V δ 2 T cell, 1-MT, and combination of V γ 9V δ 2 T cells and 1-MT group. At the indicated time for each experiment, 10^7 V γ 9V δ 2 T cells in 200 μ L of PBS were adoptively systemically transferred into tumor-bearing (50 mm³) mice by tail vein injection. Mice (control group) drank 4–5 mL H₂O/day, similar to the sum of water consumed without drug. 1-MT was administered in the drinking water for 3 weeks, starting at day 7 after tumor challenge (the fresh drinking water containing L-1MT was replaced for four times at 4-day intervals). Tumor size was measured every 2 or 3 days with a caliper, and the tumor volume was calculated using the following equation: $TV = \frac{L \times W^2}{2}$ (W=width, and L=length). Mice were sacrificed when the tumor volume reached a size of 1500 mm³. All animal experiments were independently repeated three times.

Western Blotting

MDA-MB-231 or MCF-7 cells were treated with the culture medium of V γ 9V δ 2 T cells or IFN- γ for 6, and 12 hours, and then pretreatment tumor cell lines were lysed in RIPA buffer (1 mM PMSF and complete protease inhibitor cocktail, Beyotime; Bimake) at ice for 30 minutes. After centrifugation at 13000 rpm for 15 minutes at 4°C, the supernatants were boiled for 10 minutes at 100°C. Samples were run on 12% SDS-PAGE gel, and then transferred to PVDF membranes, followed by blockade with 5% bovine serum albumin (BSA) for 2 hours at room temperature. PVDF membranes were incubated with indicated primary antibody overnight at 4°C. The following primary antibodies were used:

Primary antibodies: p-STAT1 (CST), p-NF- κ B (CST), IDO1 (CST), and β -actin (CST) were purchased from Cell Signaling Technology. After the membranes were washed in TBST for five times, they were incubated with HRP-linked secondary antibody at a dilution of 1:3,000 (CST) at room temperature for 2 hours

and were detected with the Bio-Rad ChemiDoc MP Gel imaging system (Bio-Rad).

Immunohistochemistry Staining

Paraffin-embedded clinical Luminal A and TNBC specimens were obtained from the First Affiliated Hospital, Jinan University (Guangzhou, China). PD-L1 and IDO1 staining was performed according to the protocol described in previous study (41). In brief, Tissues were incubated with anti-PD-L1 (CST) and anti-IDO1 (CST) antibody at 4°C overnight. Sections were rinsed with PBS and incubated with goat anti-rabbit antibody for 1 hour. Finally, slides were further developed with DAB substrate and then counterstained with Mayers hematoxylin.

Enzyme-Linked Immunosorbent Assay (ELISA)

Cell culture supernatant were collected, and the concentration of kynurenine was measured with ELISA kits in accordance with the manufacturer's instructions (Bioswamp). In brief, V γ 9V δ 2 T cells (effector) were co-incubated with breast cancer cells (target) at different effector:target (E:T) ratios (0:1, 1:1, 5:1, and 15:1) at 37°C for 12 hours (tumor cells number = 2.5×10^5). In some experiments, the breast cancer and V γ 9V δ 2 T cells were treated with 0.5 mM 1-methyl-DL-tryptophan (Sigma-Aldrich) for 12 hours. Co-incubation meant that residual 1-MT in the medium was not washed out and remained in the subsequent experiment. Lastly, the cell culture mixture was centrifuged, and the culture supernatant was collected to clean tubes for standard kynurenine measurement.

Data Availability

The single-cell RNA-sequencing data that support the findings of this study were available from Expression Atlas: <https://www.ebi.ac.uk/gxa/sc/experiments>. The data of single-cell RNA-sequencing was obtained from Single-cell RNA-seq enables comprehensive tumor and immune cell profiling in primary breast cancer (42), and illustrated by the tool of Single Cell Expression Atlas (43). The levels of *PD-L1* and *IDO1* in breast cancer were displayed as CPM (counts per million) and broken down into four different, logarithmic color ranges: Grey spot: expression level was below cutoff (0.1 CPM) or undetected; Light blue spot: expression level was low (between 0.1 to 10 CPM); Medium blue spot: expression level was medium (between 11 to 1000 CPM); Dark blue spot: expression level was high (more than 1000 CPM). The RNA-Seq dataset that support the conclusions of this article are available from GEPIA: <http://gepia2.cancer-pku.cn/#index>. The RNA-Seq datasets GEPIA was based on the UCSC Xena project (<http://xena.ucsc.edu/>), which were computed by a standard pipeline. Linear regression analysis between PD-L1 (CD274) and IDO1 in human breast cancer samples from the TCGA dataset (BRCA cases, $n=1085$), and linear regression analysis were performed using Pearson (44). GEPIA was also applied to evaluate the overall survival (OS) and diseases-free survival (DFS) of patients with high or low CD274 (PD-L1) expression in Luminal A [n (high)=205, n (low)=205] and TNBC [n (high)=67, n (low)=67]. The cutoff was defined as: Group

Cutoff (Median), Cutoff-High (%) and Cutoff-Low (%) =50, and survival analysis based on the expression status of PD-L1 signature and plot a Kaplan-Meier curve. Box plots showed the level of signatures gene set in cancer tissues and para-cancerous tissue with TNBC and Luminal A subtypes. Signatures Gene Set: Naïve T-cell (*CCR7*, *LEF1*, *TCF7*, and *SELL*), effector T-cell (*CX3CR1*, *FGFBP2*, and *FCGR3A*), central memory T-cell (*CCR7*, *SELL*, and *IL7R*), exhausted T-cell (*HAVCR2*, *TIGIT*, *LAG3*, and *PDCD1*), and resting Treg T-cell (*FOXP3* and *IL2RA*), or the specific gene indicated as *IDO1*. (TNBC, $n=135$; luminal A, $n=415$; para-cancerous tissues, $n=291$). The Log_2^{FC} Cutoff = 1, and the p-value Cut off = 0.01. For pathological stage plot analysis, GEPIA used major stage (yes) or sub-stage (no) for plotting. Log scale defined as $\log_2(\text{TPM}+1)$ for log-scale by GEPIA database.

Statistical Analysis

Statistical analyses were performed using GraphPad Prism 6.0 (GraphPad Software). Where indicated, data were analyzed for statistical significance and reported as p-values. Data were analyzed by two-tailed Student's *t* test when comparing means of two independent groups and two-way ANOVA when comparing more than two groups. For sample sizes of $n > 3$, the data distribution was first checked using a Kolmogorov-Smirnov test. If the data fitted a normal distribution, a two-tailed unpaired Student's *t*-test was used when variances were similar, whereas a two-tailed unpaired Student's *t*-test with Welch's correction was used when variances were different. If the data did not fit a normal distribution, a Mann-Whitney U-test was used. $P < 0.05$ was considered statistically significant (*, $P < 0.05$; **, $P < 0.01$; ***, $P < 0.001$; and ****, $P < 0.0001$, *n.s.*, not significant). Data were presented as the mean \pm SD.

RESULTS

IDO1 and PD-L1 Were Co-Expressed in Triple-Negative Breast Cancer Samples

Tumor cells evaded immune surveillance by expressing immunosuppressive factors, such as PD-L1 and *IDO1* (15). We analyzed the levels of *PD-L1* and *IDO1* in all subtypes of breast cancer and found that expression of *IDO1* in cancer tissues were higher in para-cancerous tissues at basal like (TNBC) positive breast cancer (Figure 1A) from the Gene Expression Profiling Interactive Analysis (GEPIA) (44). Compared with other subtypes, Luminal A cancer had the lowest expression of *PD-L1* (Figure 1B) and *IDO1*, suggesting that *IDO1* may play important role in TNBC but not Luminal A cancers. We further examined the expression of *IDO1* and *PD-L1* in breast cancer patients by analyzing single-cell RNA-sequencing data from The Single Cell Expression Atlas. The results showed that the level of *PD-L1* and *IDO1* were higher in TNBC than that in Luminal A positive breast cancer (42, 43) (Supplementary Figure 1). The results of immunohistochemical staining further validated that protein levels of PD-L1 and *IDO1* were higher in patients with TNBC than that with Luminal A subset (Figure 1C). The most

commonly used representative TNBC cell line was MDA-MB-231, and the most commonly used Luminal A cell line was MCF7. Flow cytometric analysis confirmed that PD-L1 was highly expressed on MDA-MB-231 cell line (Figure 1D). The RNA-sequencing data from the Gene Expression Profiling Interactive Analysis (GEPIA) (44) revealed that expression of *PD-L1* was positively correlated with that of *IDO1* in breast cancer patients (Figure 1E). Moreover, the percentage of $\text{V}\gamma 9\text{V}\delta 2^+\text{CD}3^+$ T cells in PBMCs of TNBC patients was significantly lower than that of healthy controls (Figure 1F). However, the level of PD-L1 has no significant correlation with overall survival advantage and diseases-free survival for patients with TNBC and Luminal A subtypes (Figures 1G, H). These data indicated that *IDO1* and PD-L1 expressed and were significantly higher in TNBC than in Luminal A positive breast cancer. However, the biomarkers to predict responses to ICIs in breast cancer patients remain debatable and urgently need to be clarified.

Immune Checkpoint Receptors Were Highly Expressed on $\text{V}\gamma 9\text{V}\delta 2$ T Cells in Triple-Negative Breast Cancer Patients

$\text{V}\gamma 9\text{V}\delta 2$ T cells are another type of cytotoxic T cells important for tumor surveillance in human, besides $\text{CD}8^+$ T lymphocytes. When exploring the immune status of breast cancer patients, we found that immune exhaustion and T reg phenotypes in TNBC samples were higher than that in luminal A subtypes from the GEPIA data (44) (Figures 2A, B). In order to investigate the status of $\text{V}\gamma 9\text{V}\delta 2$ T cells in human TNBC, we recruited 30 patients with advanced TNBC and 30 healthy volunteers. The expression of immune checkpoint receptors on $\text{V}\gamma 9\text{V}\delta 2$ T cells from the peripheral blood mononuclear cells (PBMCs) was analyzed. The characteristics of the healthy volunteers and patients were summarized in Table 1. The TNBC $\text{V}\gamma 9\text{V}\delta 2^+$ T cells showed immune exhaustion phenotype as represented by the increased expression of PD-1, TIGIT, and Tim-3, while cell surface CD28 expression was insignificantly changed (Figures 2C-F and Supplementary Figure 2). The $\text{V}\gamma 9\text{V}\delta 2$ T cells from the TNBC patients produced less amounts of IFN- γ and TNF- α , whereas Granzyme B and Perforin expression were marginally reduced, when stimulated with phorbol 12-myristate 13-acetate and ionomycin *in vitro*, compared with those from healthy donors (Figures 2G-J and Supplementary Figure 3). These results revealed that the quality of $\text{V}\gamma 9\text{V}\delta 2$ T cells in TNBC patients was attenuated. This phenomenon might be due to the increased ICI level on these cells.

$\text{V}\gamma 9\text{V}\delta 2$ T Cells Could Kill Breast Cancer Cells and Restrain Cancer Growth, But Without Enhanced Function With Anti-PD-L1 Addition

Recent clinical studies demonstrated the safety and efficacy of allogeneic $\text{V}\gamma 9\text{V}\delta 2$ T-cell immunotherapy (32). On this basis, we hypothesized that combination of $\text{V}\gamma 9\text{V}\delta 2$ T cells and anti-PD-L1 might be important for TNBC immunosurveillance and might help restrain cancer growth. To address this question,

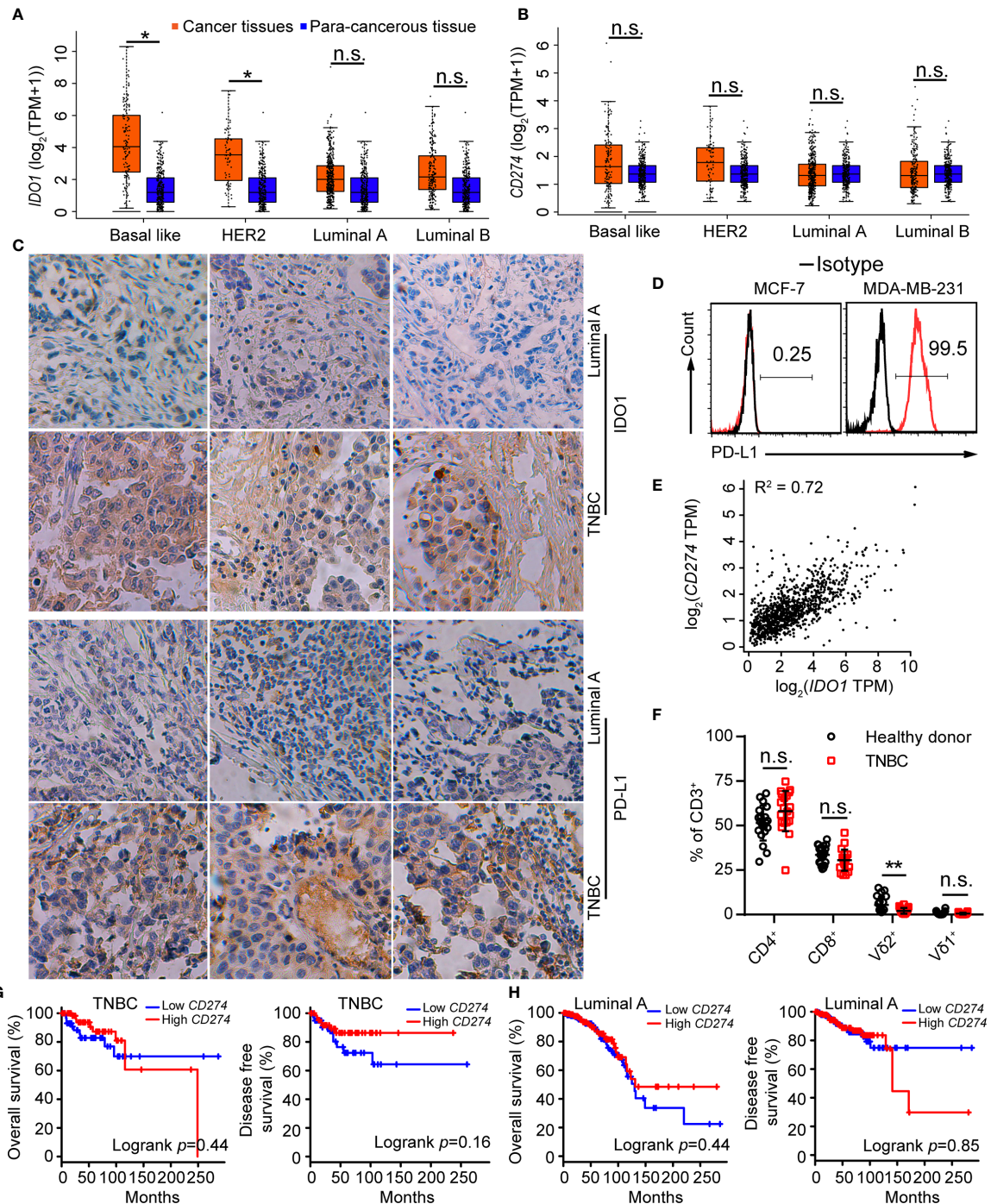


FIGURE 1 | IDO1 and PD-L1 were co-expressed in triple-negative breast cancers. **(A, B)** Expression of *IDO1* and *PD-L1* in breast cancers from the GEPIA dataset (Basal like, Cancer tissues ($n=135$); HER2, Cancer tissues ($n=66$); Luminal A, Cancer tissues ($n=415$); Luminal B, Cancer tissues ($n=194$); para-cancerous tissues, $n=291$). Cancer tissues (orange box) labeled as “tumor” were compared with para-cancerous tissues (blue box) labeled as “normal”. Immunohistochemistry **(C)** for IDO1 and PD-L1 expression in cancer tissues with luminal A and TNBC ($n=3$). **(D)** Representative histograms of PD-L1 expression by MCF-7 (luminal A) and MDA-MB-231 (TNBC) cells. **(E)** Correlation between *PD-L1* and *IDO1* expression in human breast cancer samples from the GEPIA ($n=1085$; $R^2 =$ values by linear regression). **(F)** Dot plots showing T cell subsets isolated from healthy or patient donors with TNBC PBMCs, expressed as percentage of CD3⁺ cells ($n=20$). **(G)** Overall survival and disease-free survival of triple-negative breast cancer patients with high or low *CD274* (*PD-L1*) expression (n (high)=67, n (low)=67) as defined by the median. Compared by log-rank (Mantel-Cox) test (GEPIA data base). **(H)** Overall survival and disease-free survival of luminal A breast cancer patients with high or low *CD274* (*PD-L1*) expression (n (high)=205, n (low)=205) as defined by the median. Compared by log-rank (Mantel-Cox) test (GEPIA data base). Unpaired Student’s *t*-test (F). Significance was set to $P < 0.05$ and represented as * $P < 0.05$, ** $P < 0.01$, *** $P < 0.001$, and **** $P < 0.0001$, *n.s.*, not significant.

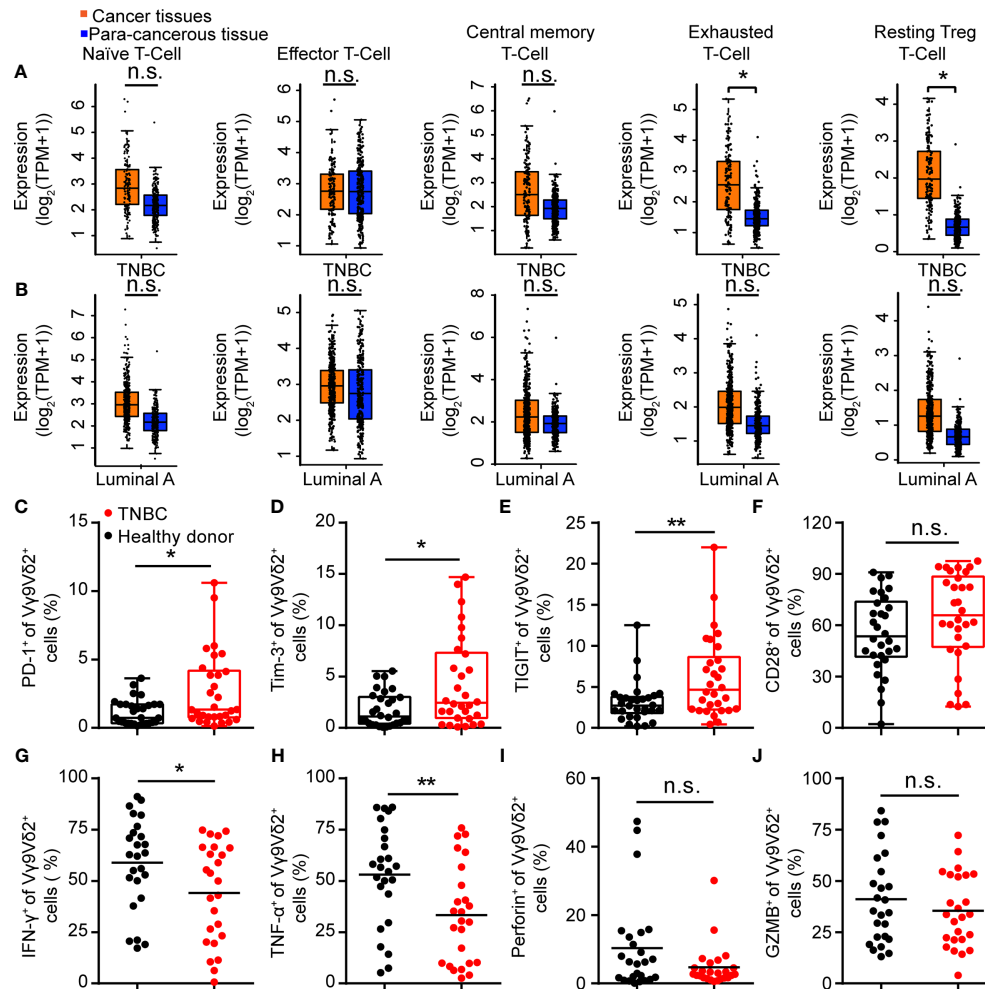


FIGURE 2 | Immune checkpoint receptors were highly expressed on Vγ9Vδ2 T cells in triple negative breast cancer patients. **(A, B)** Expression of T cell function-associated genes in TNBC and luminal A cancers from the GEPIA dataset (TNBC, $n=135$, luminal A, $n=415$). Cancer tissues (orange box) were compared with para-cancerous tissues (blue box, $n=291$). Signatures Gene Set: Naïve T-cell (*CCR7*, *LEF1*, *TCF7*, and *SELL*), effector T-cell (*CX3CR1*, *FGFBP2*, and *FCGR3A*), central memory T-cell (*CCR7*, *SELL*, and *IL7R*), exhausted T-cell (*HAVCR2*, *TIGIT*, *LAG3*, and *PDCD1*), and resting Treg T-cell (*FOXP3* and *IL2RA*). The method for differential analysis was one-way ANOVA, using disease state (Tumor or Normal) as variable for calculating differential expression **(A, B)**. **(C–F)** Expression of PD-1⁺ **(C)**, Tim-3⁺ **(D)**, TIGIT⁺ **(E)**, and CD28⁺ **(F)** on Vγ9Vδ2 T cells in healthy donors ($n=30$) and triple negative breast cancer patients ($n=30$). **(G–J)** Percentage of Vγ9Vδ2 T cells producing IFN-γ⁺ **(G)**, TNF-α⁺ **(H)**, Perforin⁺ **(I)**, and Granzyme B⁺ **(J)** in total Vγ9Vδ2 T cells were from patients with TNBC ($n=25$) and healthy donors ($n=25$), and stimulated with 50 ng/mL phorbol 12-myristate 13-acetate (PMA) and 1 μg/mL ionomycin (Ion) *in vitro*. Unpaired Student's *t*-test **(F–H, J)**; Mann-Whitney test **(C–E, I)**. Significance was set to $P < 0.05$ and represented as * $P < 0.05$, ** $P < 0.01$, *** $P < 0.001$, and **** $P < 0.0001$, n.s., not significant.

we expanded Vγ9Vδ2 T lymphocytes by culturing human PBMCs from healthy donors *in vitro*. Zoledronate (ZOL)-expanded Vγ9Vδ2 T cells typically accounted for more than 90% of the cultured PBMCs (**Supplementary Figure 4A**). These cells were mainly effector memory T cells (CD27⁺CD45RA⁺), which showed efficient cytotoxic activity and the potential for cytokine production (**Figure 3A** and **Supplementary Figure 4B**). The purity of the enriched Vγ9Vδ2 T cells was validated by flow cytometry and was generally higher than 95% (**Supplementary Figure 4C**). Flow cytometric analysis confirmed that the ZOL-expanded Vγ9Vδ2 T lymphocytes *in vitro* induced NKG2D expression, whereas the level of PD-1 marginally increased, suggesting that ZOL-expanded Vγ9Vδ2 T

cells were suitable for further adoptive immunotherapy (**Supplementary Figures 4D, E**). The frequency of viable Vγ9Vδ2 T cells (annexin-V⁻/PI⁻), early apoptotic cells (annexin-V⁺/PI⁻), and late apoptotic cells (annexin-V⁺/PI⁺) was analyzed by flow cytometry (**Figure 3B**). The ZOL-expanded Vγ9Vδ2 T cells showed few annexin-V⁺/PI⁺ population when cultured to day 20, thereby suggesting that long-term-expanded Vγ9Vδ2 T cells had sustained anti-apoptotic ability *in vitro*. We performed killing assay by using breast cancer cells co-cultured with Vγ9Vδ2 T cells *in vitro* to investigate whether Vγ9Vδ2 T cells could inhibit the growth of breast cancer cells. The proportion of apoptotic cells in MCF-7 (Luminal A) was generally higher than that in MDA-MB-231

TABLE 1 | Information of TNBC patients and healthy donors.

Patient characteristics					Healthy donor characteristics		
Case ID	Gender	Age	Types of cancer	Stage at diagnosis	Case ID	Gender	Age
1	female	61	Triple-negative breast cancer	IV	1	female	51
2	female	48	Triple-negative breast cancer	IV	2	female	40
3	female	63	Triple-negative breast cancer	IV	3	female	66
4	female	58	Triple-negative breast cancer	IV	4	female	65
5	female	46	Triple-negative breast cancer	IV	5	female	55
6	female	64	Triple-negative breast cancer	IV	6	female	52
7	female	67	Triple-negative breast cancer	IV	7	female	48
8	female	54	Triple-negative breast cancer	III	8	female	68
9	female	59	Triple-negative breast cancer	III	9	female	57
10	female	38	Triple-negative breast cancer	IV	10	female	68
11	female	44	Triple-negative breast cancer	IV	11	female	32
12	female	57	Triple-negative breast cancer	IV	12	female	77
13	female	55	Triple-negative breast cancer	IV	13	female	56
14	female	63	Triple-negative breast cancer	III	14	female	55
15	female	65	Triple-negative breast cancer	IV	15	female	63
16	female	67	Triple-negative breast cancer	IV	16	female	67
17	female	70	Triple-negative breast cancer	IV	17	female	69
18	female	66	Triple-negative breast cancer	IV	18	female	55
19	female	54	Triple-negative breast cancer	IV	19	female	51
20	female	68	Triple-negative breast cancer	IV	20	female	49
21	female	55	Triple-negative breast cancer	III	21	female	55
22	female	47	Triple-negative breast cancer	III	22	female	75
23	female	33	Triple-negative breast cancer	III	23	female	43
24	female	67	Triple-negative breast cancer	IV	24	female	37
25	female	82	Triple-negative breast cancer	IV	25	female	39
26	female	65	Triple-negative breast cancer	IV	26	female	78
27	female	54	Triple-negative breast cancer	IV	27	female	65
28	female	39	Triple-negative breast cancer	IV	28	female	63
29	female	47	Triple-negative breast cancer	IV	29	female	59
30	female	66	Triple-negative breast cancer	III	30	female	68

(TNBC) when they were treated with V γ 9V δ 2 T cell alone; meanwhile, the combination of V γ 9V δ 2 T cells and anti-PD-L1 could not further enhance the killing efficacy (**Figures 3C–E** and **Supplementary Figures 5A, B**). In a tumor-bearing mouse model, no obvious difference of tumor size shrinkage was observed under the therapy of V γ 9V δ 2 T cells combined with anti-PD-L1, compared with that of V γ 9V δ 2 T cells alone (**Figures 3F, G**). In summary, these results showed that V γ 9V δ 2 T cells could kill breast cancer cells; however, anti-PD-L1 antibody did not obviously contribute to promote the antitumor function of these cells.

IDO1 Inhibitor 1-MT Enhanced the Antitumor Efficacy of V γ 9V δ 2 T Cells

Based on these observations, we assumed that IDO1 co-expressed with PD-L1 might be involved in regulating the antitumor activity of V γ 9V δ 2 T cells. Accordingly, we examined the level of *IDO1* in breast cancer samples by using RNA-sequencing data from GEPIA (44). The analysis results showed that it differently expressed in different pathological stages (**Figure 4A**). We detected the expression of pSTAT1 and found that pSTAT1 expression positively correlated with IDO1 expression and was IFN- γ dose-dependent in MDA-MB-231 cell lines (**Figure 4B**). The expression of IDO1 enzyme in MDA-MB-231 cells was induced by IFN- γ and the culture supernatant of activated

V γ 9V δ 2 T cells, while it was barely detectable in MCF-7 cells (**Figure 4C**). This finding suggested that the upregulated expression of IDO1 in MDA-MB-231 cells might depend on the IFN- γ -pSTAT1 signaling pathway (2). Then we conducted a killing experiment *in vitro* to further validate whether IDO1 enzyme activity was involved in regulating the antitumor function of V γ 9V δ 2 T cells. The MDA-MB-231 cells were co-cultured with V γ 9V δ 2 T cells according to the designated E (effector, V γ 9V δ 2 T cell): T (target, tumor cell) ratios. The result showed that kynurenine level were significantly reduced by IDO1 enzyme inhibitor 1-MT (**Figure 4D**). The proportion of apoptotic MDA-MB-231 cells was higher in the group treated with V γ 9V δ 2 T cells and 1-MT or Lindrost (BMS-986205) than that in the group of V γ 9V δ 2 T cell treatment alone (**Figure 4E**; **Supplementary Figure 6A**). Moreover, 1-MT or Lindrostat treatment alone (without V γ 9V δ 2 T cells) did not increase the cell death (**Supplementary Figures 6B, C**). The NOD-scid immuno-deficient mice were inoculated with MDA-MB-231 cells to evaluate the therapeutic effects of V γ 9V δ 2 T cells and 1-MT for breast cancer. Seven days later, the mice were treated with V γ 9V δ 2 T cells and/or 1-MT. The results showed that the volume of tumors in the group treated with V γ 9V δ 2 T cells combined with 1-MT was significantly smaller than that of PBS group and groups treated with V γ 9V δ 2 T cell alone or 1-MT alone (**Figures 4F–H**). These data indicated that human V γ 9V δ 2 T cells could kill MDA-

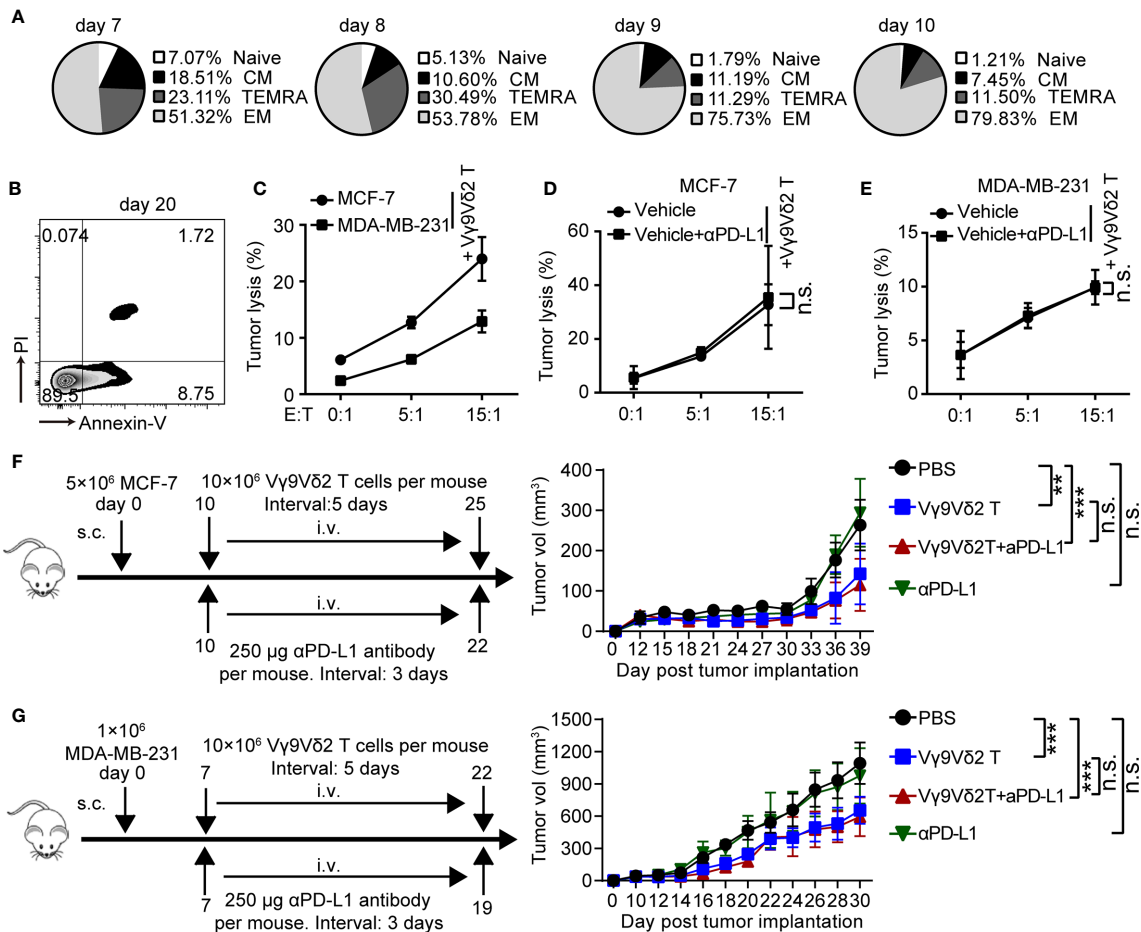


FIGURE 3 | Vγ9Vδ2 T cells could kill breast cancer cells and restrain cancer growth, but without enhanced function with anti-PD-L1 addition. **(A)** Subsets of Vγ9Vδ2 T cells cultured on day 7, 8, 9, and 10. According to the CD45RA and CD27 expression, the Vγ9Vδ2 T lymphocytes were subdivided into: CM (CD27⁺CD45RA⁺), naïve (CD27⁺CD45RA⁻), TEMRA (CD27⁻CD45RA⁺), and EM (CD27⁻CD45RA⁻). **(B)** Survival of Vγ9Vδ2 T cells cultured to day 20. Cell apoptosis (PI⁺ Annexin-V⁺) were analyzed by flow cytometry. **(C)** Cytotoxicity of Vγ9Vδ2 T cells toward breast cancer cells (MCF-7 or MDA-MB-231) at the indicated effector to target ratio (E:T). The percentages of dead cells out of whole target cells were identified as PI⁺ (n=5). **(D, E)** Cytotoxicity of Vγ9Vδ2 T cells had no obvious difference at the indicated E:T ratio with MCF-7 or MDA-MB-231 cells (target cells) pretreated with vehicle or anti-PD-L1 (10 μg/mL) for 6 hours (n=5). Dead target cells out of the total target cells were recorded. **(F, G)** Schematic protocols of tumor growth model (left). i.v., intravenous; s.c., subcutaneous. Progression of MCF-7 tumors and MDA-MB-231 tumors in mice was assessed in NOD/scid mice. n=5 mice per group. Experiments were independently repeated three times **(F, G)**. Vγ9Vδ2 T cells from healthy donors were expanded with ZOL. Data represent mean ± SD **(C-G)**. Unpaired Student's *t*-test **(C-E)**; two-way analysis of variance (ANOVA) **(F, G)**. Significance was set to *P* < 0.05 and represented as **P* < 0.05, ***P* < 0.01, ****P* < 0.001, *****P* < 0.0001, n.s., not significant.

MB-231 cells and restrain tumor growth, and the IDO enzyme inhibitor themselves could not kill breast cancer cells efficiently, but could enhance the antitumor efficacy of Vγ9Vδ2 T cells.

Treatment With 1-MT Promoted Perforin Production of Vγ9Vδ2 T Cells Under MDA-MB-231 Cell Stress

How did 1-MT enhance the antitumor function of Vγ9Vδ2 T cells in our experiment system? To address this question, we took advantage of killing system: the MDA-MB-231 or MCF-7 cells were co-cultured with Vγ9Vδ2 T cells with or without 1-MT, and the cytokine secretion in the supernatant of Vγ9Vδ2 T cells was analyzed (**Figure 5A**). The perforin production of Vγ9Vδ2 T cells treated with MCF-7 and 1-MT was not significantly more

than that of MCF-7 treatment alone. However, the production of perforin was more significantly induced in the supernatant of Vγ9Vδ2⁺ T cells treated with MDA-MB-231 cells combined with 1-MT, compared with that of MDA-MB-231 treatment alone (**Figures 5B, C**). We found that Vγ9Vδ2⁺ T cells in above co-culture system could produce cytotoxic cytokines IFN-γ, TNF-α and Granzyme B; however, no significant enhancement was observed with 1-MT treatment combination (**Figures 5D, E**). These results showed that blocking the IDO1 enzyme enhanced the cytotoxicity of Vγ9Vδ2 T cells through promoting perforin production. γδ T cells express the activating receptor NKG2D, which endows them with a TCR-independent second activation pathway *via* recognition of NKG2D ligands on tumor cells (45). So, we also detected the NKG2D expression on Vγ9Vδ2 T cells in

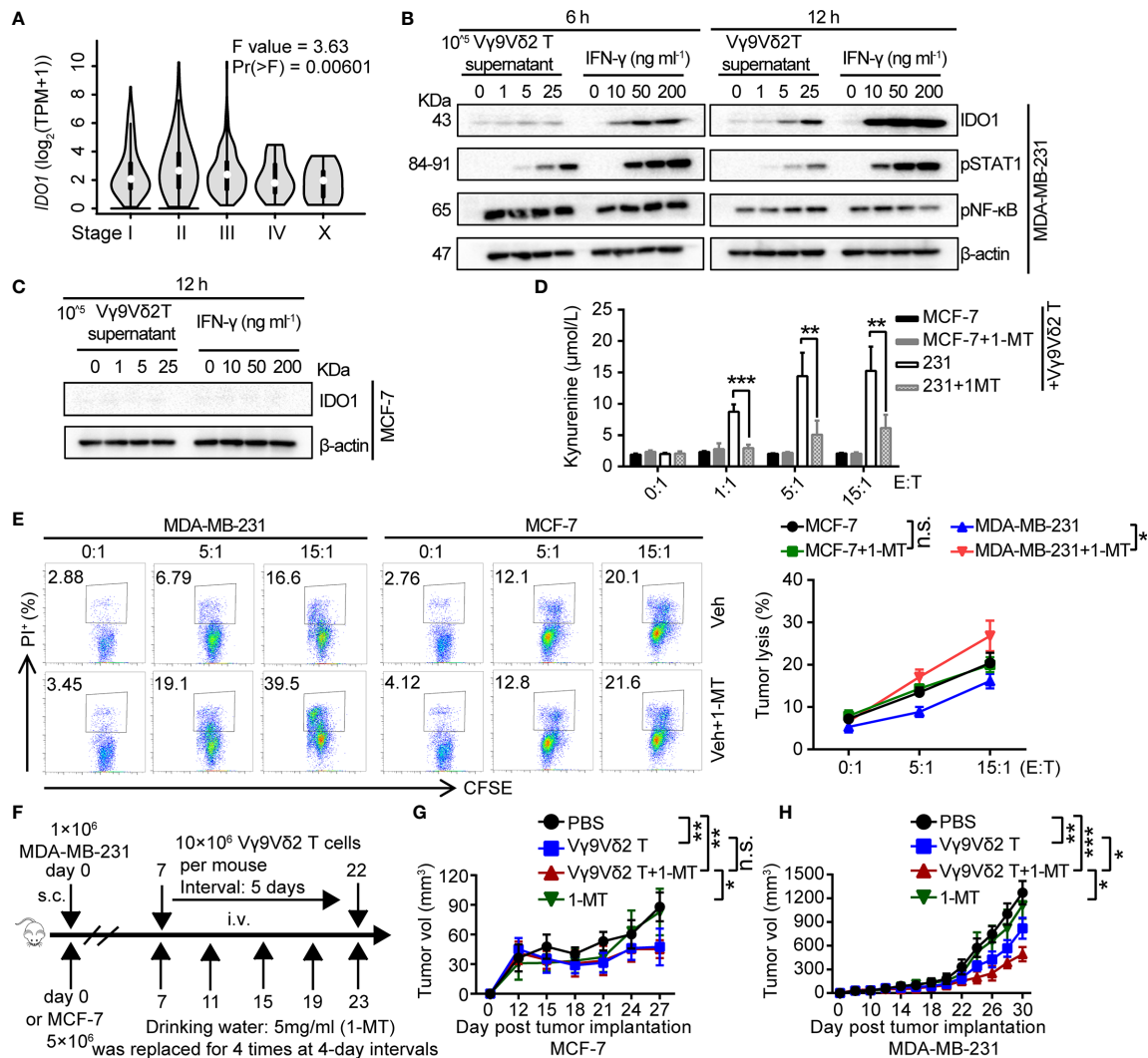


FIGURE 4 | 1-MT enhanced the antitumor efficacy of V γ 9V δ 2 T cells. **(A)** Expression of *IDO1* in BRCA at different pathological stages, (BRCA, $n=1085$). **(B)** MDA-MB-231 cells were treated with the culture medium of V γ 9V δ 2 T cells or IFN- γ for 6, and 12 hours. Western blot to detect *IDO1*, p-STAT1, and p-NF- κ B expression; β -actin was used as the loading control. **(C)** MCF-7 cells were treated with culture supernatant of V γ 9V δ 2 T cells or IFN- γ for 12 hr. Western blot to detect *IDO1* level; β -actin was used as the loading control. **(D)** Kynurenine was the metabolite of L-tryptophan catalyzed by *IDO1* enzyme, and its level in the culture supernatant of MCF-7 and MDA-MB-231 cells cocultured with V γ 9V δ 2 T cells treated with or without 1-MT was shown. The amounts of kynurenine were measured by ELISA kits. **(E)** *IDO1* inhibitor 1-MT facilitated the cytotoxicity of V γ 9V δ 2 T cells toward MDA-MB-231 cells, but not MCF-7 cells. MCF-7 or MDA-MB-231 cells (target) were co-cultured with V γ 9V δ 2 T cells (effector) with 1-MT or vehicle for 6 hours. The percentage of dead cells out of total target cells was shown. **(F–H)** Schematic protocols of tumor growth model (left). $n=5$ mice per group. Experiments were independently repeated three times **(H, I)**. Results in **(C, D)** were representative blots from 2 to 3 independent experiments. V γ 9V δ 2 T cells from healthy donors were expanded with ZOL. Data represent mean \pm SD **(E, F, H, I)**. Unpaired two-tailed Student's *t*-test **(E, F)**; one-way ANOVA using the disease state (tumor or normal) as variable for calculating the differential expression of *IDO1* **(A)**; The method for *IDO1* expression analysis was one-way ANOVA by using the pathological stage as variable for calculating differential expression **(B)**; two-way ANOVA **(H, I)**. Significance was set to $P < 0.05$ and represented as * $P < 0.05$, ** $P < 0.01$, *** $P < 0.001$, **** $P < 0.0001$, *n.s.*, not significant.

the same experimental system, but it did not significantly change (**Supplementary Figure 7**). Previous study showed a strong correlation between anticancer activity of V γ 9V δ 2 T cells and MICA/B expression on tumor cells *in vitro* (46, 47). So, we further analyzed the level of MICA/B on MDA-MB-231 and MCF-7 cells, and found that NKG2D's ligand MICA/B highly expressed on surface of MDA-MB-231 cells, however was barely detectable on MCF-7 cells (**Supplementary Figure 8**).

These results indicated that MICA/B might also be involved in the killing of MDA-MB-231 cells by V γ 9V δ 2 T cells.

DISCUSSION

Approximately 2.26 million newly diagnosed female breast cancer cases were recorded worldwide in 2020 (48). Triple-

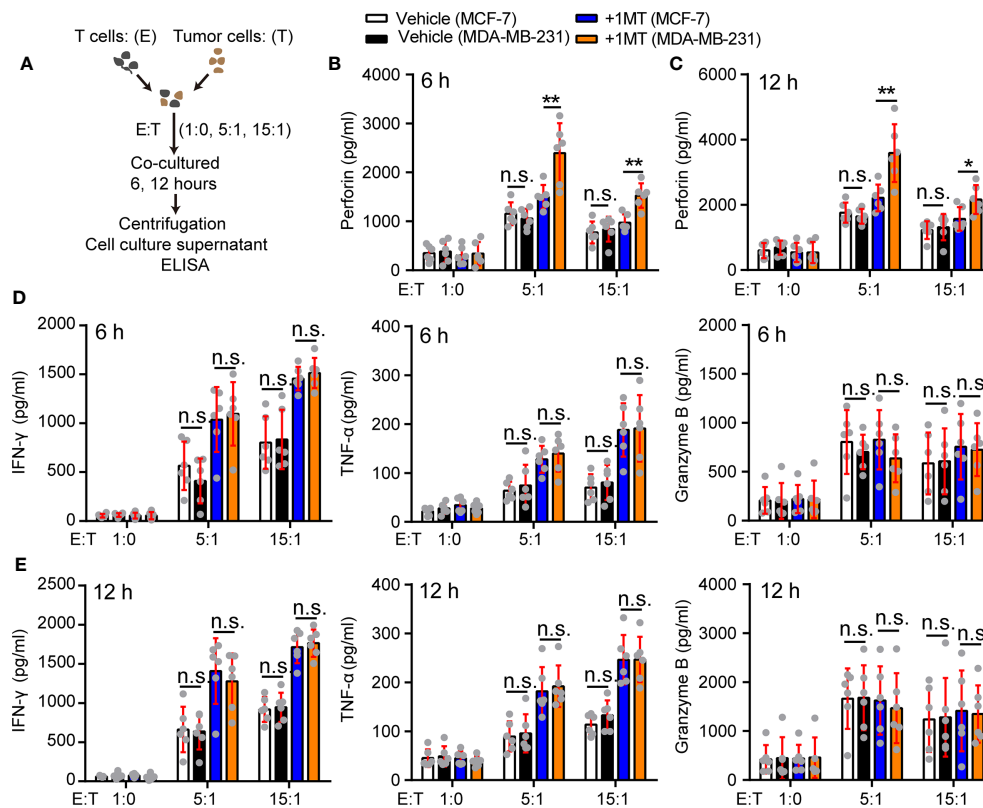


FIGURE 5 | Treatment with 1-MT and MDA-MB-231 cells enhanced perforin production of V γ 9V δ 2 T cells. **(A)** Experimental approach. **(B–E)** The levels of cytokines, released by V γ 9V δ 2 T cells, were measured by ELISA after V γ 9V δ 2 T cells from healthy donors were incubated with MCF-7 or MDA-MB-231 cells for 6 or 12 hours in the presence or absence of 1-MT (500 μ M) ($n=6$). Data represent mean \pm SD; unpaired Student's t -test **(B–E)**. Significance was set to $P < 0.05$ and represented as * $P < 0.05$, ** $P < 0.01$, *** $P < 0.001$, and **** $P < 0.0001$, n.s., not significant.

negative breast cancer is a subtype of breast cancer with the poorest prognosis due to lack of targeted therapies. Immunotherapeutic strategies for treating breast cancers had aroused great interest. Several immunotherapeutic agents had received approval of US Food and Drug Administration (FDA), including vaccines, adoptive cell therapies, oncolytic viruses, and most notably, immune checkpoint blockade (3). Our findings showed that the expression of *PD-L1* was positively correlated with *IDO1* in TNBC patients from the data of GEPIA RNA-sequencing, thereby implying that immunosuppressive effects dominated in this type of tumors and prevented normal T cell function. Gamma delta ($\gamma\delta$) lymphocyte cells infiltrated into most human tumors (49). We detected V γ 9V δ 2 T cells in blood and found that their function was suppressed, and the cell number decreased in TNBC patients. *In vitro* and *in vivo* works showed that human V γ 9V δ 2 T cells could inhibit growth of MDA-MB-231 cells, a type of TNBC cancer cells; however, the combination with anti-PD-L1 treatment could not increase their antitumor capacity. Interestingly V γ 9V δ 2 T cells combined with 1-MT, IDO1 inhibitor, enhanced their antitumor ability. Finally, we found that blocking the IDO1 enzyme enhanced the cytotoxicity of V γ 9V δ 2 T cells by perforin secretion under tumor burden stress.

IDO expression had been illustrated in tumor cells and antigen presenting cells (APC) (human monocyte-derived macrophages and dendritic cell) in a range of human cancer patients and murine cancer models (50, 51). In TNBC subtypes, IDO1 and PD-L1 were upregulated by interferon- γ -secreting T cells in the tumor microenvironment (52). However, previous clinical study showed that there was no clear evidence for benefit of adding navoximod (IDO inhibitor) to atezolizumab (PD-L1) (25). Recent work also indicated that the IDO inhibitor promoted V γ 9V δ 2 T cell's antitumor response against Ductal Pancreatic Adenocarcinoma Cells (53). The results of those studies suggested that IDO inhibitor probably targeted on human cytotoxic T cells; thus, only T cells infiltrated into tumors would have responded to the IDO inhibitor therapy (54). This finding might explain why the combination of IDO inhibitor and anti-PD-1/PD-L1 therapy did not demonstrate improved survival in many types of cancer patients. In this study, we found that only treatment of V γ 9V δ 2 T cell and 1-MT combination had more significant therapeutic effect and resulted in slower tumor growth in mouse model. This finding suggested that V γ 9V δ 2 T lymphocytes/1-MT combination might have potential applications in therapy of TNBC patients, which would inspire further clinical investigations and eventually benefit cancer patients.

IDO expression was correlated with increased tumor-infiltrating T regulatory cells (T reg); studies had suggested that tumor cells or IDO-expressing APCs could mediate T reg cells to strongly dampen the antitumor responses of T cells (16, 39). The intratumor ratio of infiltrating lymphocytes (TILs) to T reg cells was considered as a marker of favorable immunological responses, which was a possible key factor to control tumor progression (5, 55). Previous work showed that intratumoral $\gamma\delta$ T cell numbers were positively correlated with advanced tumor stages, HER2 expression status, FOXP3⁺ cells, and high lymph node metastasis, but inversely correlated with relapse-free survival and overall survival of breast cancer patients (6). However, Andrew J Gentles et al. demonstrated that intratumoral $\gamma\delta$ T cells emerged as a significant favorable marker in breast cancer survival (10). The possible reason for this contradictory phenomenon was that $\gamma\delta$ T cells played different roles in different breast cancer subtypes. T cell exhaustion was a poor responsive status with an upregulated level of ICIs, decreased production of cytotoxic cytokines, and suppressed antitumor efficacy (56). Our data showed that V γ 9V δ 2 T cells in triple-negative breast cancer patients had exhausted phenotype with increased PD-1, TIGIT, and Tim-3 expression and reduced cytokine production. These findings suggested that dysfunctional V γ 9V δ 2 T cells in triple-negative breast cancer patients might be another important factor to accelerate tumor progression besides CD8⁺ T cells.

Cytotoxic T cell exerted antitumor effects *via* cytokine production, such as IFN- γ , TNF- α , granzyme B, and perforin (49), under the specific tumor antigen stimulation. *IDO1* is a classic IFN- γ -inducible gene (57). However, in the analysis of several breast cancer datasets, previous reports showed differences of subtype-specific mRNA and promoter methylation in *IDO1*, with TNBC/basal subtypes exhibiting low methylation/higher expression phenotype and ER⁺/luminal subtypes demonstrating high methylation/lower expression phenotype (15). Those results suggested that the *IDO1* gene in TNBC cells was intrinsically open for transcription. The high expression of *IDO1* in TNBC patients could intensively inhibit V γ 9V δ 2 T cells. This phenomenon may explain our results: V γ 9V δ 2 T cells in TNBC patients expressed high levels of ICIs, such as PD-1, Tim3, and TIGIT, and produced less cytokines, such as IFN- γ and TNF- α . The immunosuppressed V γ 9V δ 2 T cells were relieved to produce many cytokines when treated with the IDO inhibitor and restrained tumor growth. We also confirmed that V γ 9V δ 2 T cells treated with the IDO inhibitor promoted perforin production, but not IFN- γ and TNF- α under the tumor stress. However, IDO inhibitor mediated the transcription of perforin needs to be further investigated.

In summary, our data showed that IDO inhibitor facilitated V γ 9V δ 2 T cell antitumor activity. The combination of V γ 9V δ 2 T cells and IDO inhibitor could result in additive and strong effects for suppressing MDA-MB-231 cell growth. V γ 9V δ 2 T cells combined with IDO inhibitor might be a safe and economical approach to treat triple negative breast cancers. The efficacy of V γ 9V δ 2 T cells and IDO blockade therapy in TNBC patients need to be further validated in clinical trials.

DATA AVAILABILITY STATEMENT

The datasets presented in this study can be found in online repositories. The names of the repository/repositories and accession number(s) can be found below: The Expression Atlas database <https://www.ebi.ac.uk/gxa/sc/experiments> under the accession number SRP066982.

ETHICS STATEMENT

The studies involving human participants were reviewed and approved by The Institutional Review Board of Jinan University, Guangzhou, P. R. China. The patients/participants provided their written informed consent to participate in this study. The animal study was reviewed and approved by The Jinan University Institutional Laboratory Animal Care and Use Committee.

AUTHOR CONTRIBUTIONS

YG and PeL conceived the project and designed the study. PeL, RW, and KL wrote the manuscript, made the figures. PeL and RW performed research. JZ, WY, XZ, YZ, PiL, CZ, and XW provided technical assistance. PeL and YG discussed and interpreted the data. PeL, KL, and RW contributed to manuscript preparation. All authors contributed to the article and approved the submitted version.

FUNDING

This work was supported by the National Natural Science Foundation of China (grant 31770964 to YG) and the 111 Project (grant B16021 to YG).

SUPPLEMENTARY MATERIAL

The Supplementary Material for this article can be found online at: <https://www.frontiersin.org/articles/10.3389/fonc.2021.679517/full#supplementary-material>

Supplementary Figure 1 | The levels of *PD-L1* and *IDO1* in TNBC and Luminal A breast cancers. (A) t-SNE plot of all 515 classified cells, demonstrating separation by cell type. Individual cells were colored green for luminal A, yellow for luminal B, blue for HER2, and red for TNBC tumors (The Single Cell Expression Atlas data base). (B) Expression levels of *IDO1* and *PD-L1* across 515 single cells illustrated in t-SNE plots. Individual cells were colored red for TNBC, blue for luminal A (The Single Cell Expression Atlas data base).

Supplementary Figure 2 | Identification of exhaustion and costimulatory markers in triple negative breast cancer patients. PD-1⁺, Tim-3⁺, TIGIT⁺, and CD28⁺ levels on V γ 9V δ 2⁺ T cells in PBMCs of healthy donors and triple negative breast cancer patients (TNBC) were shown.

Supplementary Figure 3 | Cytokine production of V γ 9V δ 2⁺ T cells. Frequency of TNF- α ⁺, IFN- γ ⁺, Perforin⁺, and Granzyme B⁺ V γ 9V δ 2⁺ T cells in healthy donor and triple negative breast cancer samples were shown.

Supplementary Figure 4 | Percentage of NKG2D⁺, PD-1⁺ Vγ9Vδ2 T cells out of the total Vγ9Vδ2 T lymphocyte population. **(A, B)** Representative flow cytometry plots showing the gating strategy to identify lymphocytes including subsets of Vγ9Vδ2 T cells expanded from ZOL. **(C)** Vγ9Vδ2 T cells were further purified by negative selection with EasySep™ Human Gamma/Delta T Cell Isolation Kit. **(D, E)** Vγ9Vδ2 T cells were expanded *in vitro* from the human peripheral blood cells with ZOL. Frequency of NKG2D and PD-1 expression on Vγ9Vδ2⁺ T cells at day 12 was shown.

Supplementary Figure 5 | Anti-PD-L1 antibody could not further enhance the antitumor efficacy of Vγ9Vδ2 T cells. **(A)** Cytotoxicity of Vγ9Vδ2 T cells toward MCF-7 or MDA-MB-231 cell lines at the indicated ratio of effector to target (E:T). Frequency of dead cells out of whole target cells were showed as PI⁺. **(B)** Cytotoxicity of Vγ9Vδ2 T cells had no obvious difference at the indicated E:T ratio with MCF-7 or MDA-MB-231 cells (target cells) pretreated with anti-PD-L1 (10 μg/mL) or not for 6 hours. Dead target cells out of the total target cells were determined.

Supplementary Figure 6 | 1-MT treatment alone did not induce tumor cell apoptosis. **(A)** IDO1 inhibitor Lindrostat facilitated the cytotoxicity of Vγ9Vδ2 T cells against MDA-MB-231 cells, but not MCF-7 cells. MCF-7 or MDA-MB-231 cells

(target) were co-cultured with Vγ9Vδ2 T cells (effector) with Lindrostat or vehicle for 6 hours. The percentage of dead cells out of total target cells was shown. *n*=3.

(B, C) MCF-7 and MDA-MB-231 cells were treated with 1-MT (500 μM), Lindrostat (10, 100, 1000 nM) or vehicle for 6 or 12 hours. Apoptotic cells (PI⁺) were detected by flow cytometry. The data were representative of three independent experiments. Data represented mean ± SD; unpaired Student's *t*-test. Significance was set to *P* < 0.05 and represented as **P* < 0.05, ***P* < 0.01, ****P* < 0.001, and *****P* < 0.0001, *n.s.*, not significant.

Supplementary Figure 7 | 1-MT treatment did not promote NKG2D expression of Vγ9Vδ2 T cells stimulated with MDA-MB-231 cells or MCF-7 cells. Human Vγ9Vδ2 T cells co-cultured with MCF-7 or MDA-MB-231 cells were treated with 1-MT (500 μM) or vehicle for 6 hours. Expression of NKG2D on Vγ9Vδ2 T cells from healthy donors was shown (*n*=3). Data represented mean ± SD; unpaired Student's *t*-test. Significance was set to *P* < 0.05 and represented as **P* < 0.05, ***P* < 0.01, ****P* < 0.001, and *****P* < 0.0001, *n.s.*, not significant.

Supplementary Figure 8 | MICA/B levels on MDA-MB-231 and MCF-7 cells. Representative histograms of MICA/B expression by MCF-7 (luminal A) and MDA-MB-231 (TNBC) cells.

REFERENCES

- Shi P, Liu W, Tala, Wang H, Li F, Zhang H, et al. Metformin Suppresses Triple-Negative Breast Cancer Stem Cells by Targeting KLF5 for Degradation. *Cell Discov* (2017) 3:17010. doi: 10.1038/celldisc.2017.10
- Bianchini G, Balko JM, Mayer IA, Sanders ME, Gianni L. Triple-Negative Breast Cancer: Challenges and Opportunities of a Heterogeneous Disease. *Nat Rev Clin Oncol* (2016) 13(11):674–90. doi: 10.1038/nrclinonc.2016.66
- Adams S, Gatti-Mays ME, Kalinsky K, Korde LA, Sharon E, Amiri-Kordestani L, et al. Current Landscape of Immunotherapy in Breast Cancer: A Review. *JAMA Oncol* (2019) 5(8):1205–14. doi: 10.1001/jamaoncol.2018.7147
- Nanda R, Chow LQ, Dees EC, Berger R, Gupta S, Geva R, et al. Pembrolizumab in Patients With Advanced Triple-Negative Breast Cancer: Phase Ib KEYNOTE-012 Study. *J Clin Oncol* (2016) 34(21):2460–7. doi: 10.1200/JCO.2015.64.8931
- Mahmoud SM, Paish EC, Powe DG, Macmillan RD, Grainge MJ, Lee AH, et al. Tumor-Infiltrating CD8⁺ Lymphocytes Predict Clinical Outcome in Breast Cancer. *J Clin Oncol* (2011) 29(15):1949–55. doi: 10.1200/JCO.2010.30.5037
- Ma C, Zhang Q, Ye J, Wang F, Zhang Y, Wevers E, et al. Tumor-Infiltrating Gammadelta T Lymphocytes Predict Clinical Outcome in Human Breast Cancer. *J Immunol* (2012) 189(10):5029–36. doi: 10.4049/jimmunol.1201892
- Hidalgo JV, Bronsert P, Orłowska-Volk M, Diaz LB, Stickeler E, Werner M, et al. Histological Analysis of Gammadelta T Lymphocytes Infiltrating Human Triple-Negative Breast Carcinomas. *Front Immunol* (2014) 5:632. doi: 10.3389/fimmu.2014.00632
- Dadi S, Chhangawala S, Whitlock BM, Franklin RA, Luo CT, Oh SA, et al. Cancer Immunosurveillance by Tissue-Resident Innate Lymphoid Cells and Innate-Like T Cells. *Cell* (2016) 164(3):365–77. doi: 10.1016/j.cell.2016.01.002
- Badve S, Dabbs DJ, Schnitt SJ, Baehner FL, Decker T, Eusebi V, et al. Basal-Like and Triple-Negative Breast Cancers: A Critical Review With an Emphasis on the Implications for Pathologists and Oncologists. *Mod Pathol* (2011) 24(2):157–67. doi: 10.1038/modpathol.2010.200
- Gentles AJ, Newman AM, Liu CL, Bratman SV, Feng W, Kim D, et al. The Prognostic Landscape of Genes and Infiltrating Immune Cells Across Human Cancers. *Nat Med* (2015) 21(8):938–45. doi: 10.1038/nm.3909
- Chen JY, Li CF, Kuo CC, Tsai KK, Hou MF, Hung WC. Cancer/stroma Interplay *via* Cyclooxygenase-2 and Indoleamine 2,3-Dioxygenase Promotes Breast Cancer Progression. *Breast Cancer Res* (2014) 16(4):410. doi: 10.1186/s13058-014-0410-1
- Lemos H, Huang L, Prendergast GC, Mellor AL. Immune Control By Amino Acid Catabolism During Tumorigenesis and Therapy. *Nat Rev Cancer* (2019) 19(3):162–75. doi: 10.1038/s41568-019-0106-z
- Munn DH, Mellor AL. IDO in the Tumor Microenvironment: Inflammation, Counter-Regulation, and Tolerance. *Trends Immunol* (2016) 37(3):193–207. doi: 10.1016/j.it.2016.01.002
- Brandacher G, Perathoner A, Ladurner R, Schneeberger S, Obrist P, Winkler C, et al. Prognostic Value of Indoleamine 2,3-Dioxygenase Expression in Colorectal Cancer: Effect on Tumor-Infiltrating T Cells. *Clin Cancer Res* (2006) 12(4):1144–51. doi: 10.1158/1078-0432.CCR-05-1966
- Noonpalle SK, Gu F, Lee EJ, Choi JH, Han Q, Kim J, et al. Promoter Methylation Modulates Indoleamine 2,3-Dioxygenase 1 Induction by Activated T Cells in Human Breast Cancers. *Cancer Immunol Res* (2017) 5(4):330–44. doi: 10.1158/2326-6066.CIR-16-0182
- Yu J, Du W, Yan F, Wang Y, Li H, Cao S, et al. Myeloid-Derived Suppressor Cells Suppress Antitumor Immune Responses Through IDO Expression and Correlate With Lymph Node Metastasis in Patients With Breast Cancer. *J Immunol* (2013) 190(7):3783–97. doi: 10.4049/jimmunol.1201449
- Fallarino F, Grohmann U, You S, McGrath BC, Cavener DR, Vacca C, et al. The Combined Effects of Tryptophan Starvation and Tryptophan Catabolites Down-Regulate T Cell Receptor Zeta-Chain and Induce a Regulatory Phenotype in Naive T Cells. *J Immunol* (2006) 176(11):6752–61. doi: 10.4049/jimmunol.176.11.6752
- Godin-Ethier J, Pelletier S, Hanafi LA, Gannon PO, Forget MA, Routy JP, et al. Human Activated T Lymphocytes Modulate IDO Expression in Tumors Through Th1/Th2 Balance. *J Immunol* (2009) 183(12):7752–60. doi: 10.4049/jimmunol.0901004
- Ling W, Zhang J, Yuan Z, Ren G, Zhang L, Chen X, et al. Mesenchymal Stem Cells Use IDO to Regulate Immunity in Tumor Microenvironment. *Cancer Res* (2014) 74(5):1576–87. doi: 10.1158/0008-5472.CAN-13-1656
- Anderson AC, Joller N, Kuchroo VK. Lag-3, Tim-3, and TIGIT: Co-Inhibitory Receptors With Specialized Functions in Immune Regulation. *Immunity* (2016) 44(5):989–1004. doi: 10.1016/j.immuni.2016.05.001
- Leach DR, Krummel MF, Allison JP. Enhancement of Antitumor Immunity by CTLA-4 Blockade. *Science* (1996) 271(5256):1734–6. doi: 10.1126/science.271.5256.1734
- Gruber IV, El Yousfi S, Durr-Storzer S, Wallwiener D, Solomayer EF, Fehm T. Down-Regulation of CD28, TCR-Zeta (Zeta) and Up-Regulation of FAS in Peripheral Cytotoxic T-Cells of Primary Breast Cancer Patients. *Anticancer Res* (2008) 28(2A):779–84.
- Lob S, Konigshainer A, Rammensee HG, Opelz G, Terness P. Inhibitors of Indoleamine-2,3-Dioxygenase for Cancer Therapy: Can We See the Wood for the Trees? *Nat Rev Cancer* (2009) 9(6):445–52. doi: 10.1038/nrc2639
- Spahn J, Peng J, Lorenzana E, Kan D, Hunsaker T, Segal E, et al. Improved Anti-Tumor Immunity and Efficacy Upon Combination of the IDO1 Inhibitor GDC-0919 With Anti-PD-L1 Blockade Versus Anti-PD-L1 Alone in Preclinical Tumor Models. *J Immunother Cancer* (2015) 3(2):P303. doi: 10.1186/2051-1426-3-S2-P303
- Jung KH, LoRusso P, Burris H, Gordon M, Bang YJ, Hellmann MD, et al. Phase I Study of the Indoleamine 2,3-Dioxygenase 1 (IDO1) Inhibitor Navoximod (GDC-0919) Administered With PD-L1 Inhibitor

- (Atezolizumab) in Advanced Solid Tumors. *Clin Cancer Res* (2019) 25 (11):3220–8. doi: 10.1158/1078-0432.CCR-18-2740
26. Liu S, Lachapelle J, Leung S, Gao D, Foulkes WD, Nielsen TO. CD8+ Lymphocyte Infiltration Is an Independent Favorable Prognostic Indicator in Basal-Like Breast Cancer. *Breast Cancer Res* (2012) 14(2):R48. doi: 10.1186/bcr3148
 27. Janssen A, Villacorta Hidalgo J, Beringer DX, van Dooremalen S, Fernando F, van Diest E, et al. Gammadelta T-Cell Receptors Derived From Breast Cancer-Infiltrating T Lymphocytes Mediate Antitumor Reactivity. *Cancer Immunol Res* (2020) 8(4):530–43. doi: 10.1158/2326-6066.CIR-19-0513
 28. Fowler DW, Bodman-Smith MD. Harnessing the Power of Vdelta2 Cells in Cancer Immunotherapy. *Clin Exp Immunol* (2015) 180(1):1–10. doi: 10.1111/cei.12564
 29. Xia X, Zhou W, Guo C, Fu Z, Zhu L, Li P, et al. Glutaminolysis Mediated by MALT1 Protease Activity Facilitates PD-L1 Expression on ABC-DLBCL Cells and Contributes to Their Immune Evasion. *Front Oncol* (2018) 8:632. doi: 10.3389/fonc.2018.00632
 30. Gao Y, Yang W, Pan M, Scully E, Girardi M, Augenlicht LH, et al. Gamma Delta T Cells Provide an Early Source of Interferon Gamma in Tumor Immunity. *J Exp Med* (2003) 198(3):433–42. doi: 10.1084/jem.20030584
 31. Alnaggar M, Xu Y, Li J, He J, Chen J, Li M, et al. Allogenic Vgamma9Vdelta2 T Cell as New Potential Immunotherapy Drug for Solid Tumor: A Case Study for Cholangiocarcinoma. *J Immunother Cancer* (2019) 7(1):36. doi: 10.1186/s40425-019-0501-8
 32. Xu Y, Xiang Z, Alnaggar M, Kouakanou L, Li J, He J, et al. Allogeneic Vgamma9Vdelta2 T-Cell Immunotherapy Exhibits Promising Clinical Safety and Prolongs the Survival of Patients With Late-Stage Lung or Liver Cancer. *Cell Mol Immunol* (2020) 18(2):427–39. doi: 10.1038/s41423-020-0515-7
 33. Lin M, Zhang X, Liang S, Luo H, Alnaggar M, Liu A, et al. Irreversible Electroporation Plus Allogenic Vgamma9Vdelta2 T Cells Enhances Antitumor Effect for Locally Advanced Pancreatic Cancer Patients. *Signal Transduct Target Ther* (2020) 5(1):215. doi: 10.1038/s41392-020-00260-1
 34. Maude SL, Teachey DT, Porter DL, Grupp SA. CD19-Targeted Chimeric Antigen Receptor T-Cell Therapy for Acute Lymphoblastic Leukemia. *Blood* (2015) 125(26):4017–23. doi: 10.1182/blood-2014-12-580068
 35. Fuentes-Antras J, Guevara-Hoyer K, Baliu-Pique M, Garcia-Saenz JA, Perez-Segura P, Pandiella A, et al. Adoptive Cell Therapy in Breast Cancer: A Current Perspective of Next-Generation Medicine. *Front Oncol* (2020) 10:605633. doi: 10.3389/fonc.2020.605633
 36. Neelapu SS, Tummala S, Kebriaei P, Wierda W, Gutierrez C, Locke FL, et al. Chimeric Antigen Receptor T-Cell Therapy - Assessment and Management of Toxicities. *Nat Rev Clin Oncol* (2018) 15(1):47–62. doi: 10.1038/nrdclinonc.2017.148
 37. Khalil DN, Smith EL, Brentjens RJ, Wolchok JD. The Future of Cancer Treatment: Immunomodulation, CARs and Combination Immunotherapy. *Nat Rev Clin Oncol* (2016) 13(5):273–90. doi: 10.1038/nrdclinonc.2016.25
 38. Fessas P, Possamai LA, Clark J, Daniels E, Gudd C, Mullish BH, et al. Immunotoxicity From Checkpoint Inhibitor Therapy: Clinical Features and Underlying Mechanisms. *Immunology* (2020) 159(2):167–77. doi: 10.1111/imm.13141
 39. Ninomiya S, Narala N, Huye L, Yagyu S, Savoldo B, Dotti G, et al. Tumor Indoleamine 2,3-Dioxygenase (IDO) Inhibits CD19-CAR T Cells and Is Downregulated by Lymphodepleting Drugs. *Blood* (2015) 125(25):3905–16. doi: 10.1182/blood-2015-01-621474
 40. Kouakanou L, Xu Y, Peters C, He J, Wu Y, Yin Z, et al. Vitamin C Promotes the Proliferation and Effector Functions of Human Gammadelta T Cells. *Cell Mol Immunol* (2020) 17(5):462–73. doi: 10.1038/s41423-019-0247-8
 41. Ge GZ, Xia HJ, He BL, Zhang HL, Liu WJ, Shao M, et al. Generation and Characterization of a Breast Carcinoma Model by PyMT Overexpression in Mammary Epithelial Cells of Tree Shrew, an Animal Close to Primates in Evolution. *Int J Cancer* (2016) 138(3):642–51. doi: 10.1002/ijc.29814
 42. Chung W, Eum HH, Lee HO, Lee KM, Lee HB, Kim KT, et al. Single-Cell RNA-Seq Enables Comprehensive Tumour and Immune Cell Profiling in Primary Breast Cancer. *Nat Commun* (2017) 8:15081. doi: 10.1038/ncomms15081
 43. Papatheodorou I, Moreno P, Manning J, Fuentes AM, George N, Fexova S, et al. Expression Atlas Update: From Tissues to Single Cells. *Nucleic Acids Res* (2020) 48(D1):D77–83. doi: 10.1093/nar/gkz947
 44. Tang Z, Li C, Kang B, Gao G, Li C, Zhang Z. GEPIA: A Web Server for Cancer and Normal Gene Expression Profiling and Interactive Analyses. *Nucleic Acids Res* (2017) 45(W1):W98–W102. doi: 10.1093/nar/gkx247
 45. Bhat J, Kouakanou L, Peters C, Yin Z, Kabelaiz D. Immunotherapy With Human Gamma Delta T Cells-Synergistic Potential of Epigenetic Drugs? *Front Immunol* (2018) 9:512. doi: 10.3389/fimmu.2018.00512
 46. Benzaid I, Monkkonen H, Bonnelye E, Monkkonen J, Clezardin P. *In Vivo* Phosphoantigen Levels in Bisphosphonate-Treated Human Breast Tumors Trigger Vgamma9Vdelta2 T-Cell Antitumor Cytotoxicity Through ICAM-1 Engagement. *Clin Cancer Res* (2012) 18(22):6249–59. doi: 10.1158/1078-0432.CCR-12-0918
 47. Xiang Z, Liu Y, Zheng J, Liu M, Lv A, Gao Y, et al. Targeted Activation of Human Vgamma9Vdelta2-T Cells Controls Epstein-Barr Virus-Induced B Cell Lymphoproliferative Disease. *Cancer Cell* (2014) 26(4):565–76. doi: 10.1016/j.ccr.2014.07.026
 48. Sung H, Ferlay J, Siegel RL, Laversanne M, Soerjomataram I, Jemal A, et al. Global Cancer Statistics 2020: GLOBOCAN Estimates of Incidence and Mortality Worldwide for 36 Cancers in 185 Countries. *CA Cancer J Clin* (2021) 71(3):209–49. doi: 10.3322/caac.21660
 49. Silva-Santos B, Mensurado S, Coffelt SB. Gammadelta T Cells: Pleiotropic Immune Effectors With Therapeutic Potential in Cancer. *Nat Rev Cancer* (2019) 19(7):392–404. doi: 10.1038/s41568-019-0153-5
 50. Uyttenhove C, Pilotte L, Theate I, Stroobant V, Colau D, Parmentier N, et al. Evidence for a Tumoral Immune Resistance Mechanism Based on Tryptophan Degradation by Indoleamine 2,3-Dioxygenase. *Nat Med* (2003) 9(10):1269–74. doi: 10.1038/nm934
 51. Okamoto A, Nikaido T, Ochiai K, Takakura S, Saito M, Aoki Y, et al. Indoleamine 2,3-Dioxygenase Serves as a Marker of Poor Prognosis in Gene Expression Profiles of Serous Ovarian Cancer Cells. *Clin Cancer Res* (2005) 11(16):6030–9. doi: 10.1158/1078-0432.CCR-04-2671
 52. Mittendorf EA, Philips AV, Meric-Bernstam F, Qiao N, Wu Y, Harrington S, et al. PD-L1 Expression in Triple-Negative Breast Cancer. *Cancer Immunol Res* (2014) 2(4):361–70. doi: 10.1158/2326-6066.CIR-13-0127
 53. Jonescheit H, Oberg HH, Gonnermann D, Hermes M, Sulaj V, Peters C, et al. Influence of Indoleamine-2,3-Dioxygenase and Its Metabolite Kynurenine on Gammadelta T Cell Cytotoxicity Against Ductal Pancreatic Adenocarcinoma Cells. *Cells* (2020) 9(5). doi: 10.3390/cells9051140
 54. Spranger S, Spaapen RM, Zha Y, Williams J, Meng Y, Ha TT, et al. Up-Regulation of PD-L1, IDO, and T(regs) in the Melanoma Tumor Microenvironment Is Driven by CD8(+) T Cells. *Sci Transl Med* (2013) 5(200):200ra116. doi: 10.1126/scitranslmed.3006504
 55. Salem V, Centonze G, Cavallo F, Defilippi P, Conti L. The Crosstalk Between Tumor Cells and the Immune Microenvironment in Breast Cancer: Implications for Immunotherapy. *Front Oncol* (2021) 11:610303. doi: 10.3389/fonc.2021.610303
 56. He X, Xu C. Immune Checkpoint Signaling and Cancer Immunotherapy. *Cell Res* (2020) 30(8):660–9. doi: 10.1038/s41422-020-0343-4
 57. Taylor MW, Feng GS. Relationship Between Interferon-Gamma, Indoleamine 2,3-Dioxygenase, and Tryptophan Catabolism. *FASEB J* (1991) 5(11):2516–22. doi: 10.1096/fasebj.5.11.1907934

Conflict of Interest: The authors declare that the research was conducted in the absence of any commercial or financial relationships that could be construed as a potential conflict of interest.

Copyright © 2021 Li, Wu, Li, Yuan, Zeng, Zhang, Wang, Zhu, Zhou, Li and Gao. This is an open-access article distributed under the terms of the Creative Commons Attribution License (CC BY). The use, distribution or reproduction in other forums is permitted, provided the original author(s) and the copyright owner(s) are credited and that the original publication in this journal is cited, in accordance with accepted academic practice. No use, distribution or reproduction is permitted which does not comply with these terms.